JOURNAL OF VIROLOGY, Mar. 1986, p. 933–941
0022-538X/86/030933-09$02.00/0

Vol. 57, No. 3

Herpes Simplex Virus Amplicon: Cleavage of Concatemeric DNA Is Linked to Packaging and Involves Amplification of the Terminally Reiterated *a* Sequence

LOUIS P. DEISS AND NIZA FRENKEL*

The Department of Molecular Genetics and Cell Biology, The University of Chicago, Chicago, Illinois 60637

Received 24 July 1985/Accepted 19 November 1985

Herpes simplex virus-infected cells contain large concatemeric DNA molecules arising from replication of the viral genome. The large concatemers are cleaved to generate unit-length molecules terminating at both ends with the *a* sequence. We have used constructed defective virus vectors (amplicons) derived from herpes simplex virus to study the mechanism of cleavage of viral DNA concatemers and the packaging of viral DNA into nucleocapsids. These studies revealed that (i) a 248-base-pair *a* sequence contained the signal(s) required for cleavage-packaging, (ii) the cleavage of viral DNA concatemers was coupled to packaging, (iii) the *a* sequence contained the information required for its own amplification, and (iv) cleavage-packaging occurred by a novel process involving the amplification of the *a* sequence.

The 150-kilobase (kb) DNA genomes of herpes simplex virus type 1 (HSV-1) and HSV-2 are composed of two components, L and S, each consisting of unique sequences bracketed by inverted repeats: *ba* and *b'a'* flanking U_L, and *ca* and *c'a'* flanking U_S. The L and S components invert relative to each other, yielding four isomeric molecules (19, 20). The sequence *a*, which is directly repeated at both termini, was shown to be present in a variable number of copies within the L-S junctions and the L ends of all four isomers (10, 30). In contrast, the S ends contain a single copy of the *a* sequence. The standard virus genome can thus be represented by a_nb-U_L-$b'a'_mc'$-U_S-*ca*, where *n* and *m* vary from 1 to greater than 10.

HSV DNA replicates late postinfection via large concatemeric intermediates, which are subsequently cleaved to generate unit-length genomes (2, 3, 7, 19). Cleavage of these concatemers occurs within the terminally reiterated *a* sequences situated at the junctions between adjacent viral genomes (15). Although the number of *a* sequences at the junctions is variable, the predominant junctions contain a single *a* sequence.

Defective HSV genomes which accumulate in serially passaged virus stocks are typically composed of head-to-tail repeats, each containing a replication origin and the sequence *a* (5). The array of tandemly repeated units separated by junctions containing *a* sequences closely resembles the concatemeric structure of replicative intermediates of standard virus DNA. Like their standard virus counterparts, defective genomes present in cytoplasmic mature virus were shown to terminate specifically with *a* sequences (11, 29). Furthermore, for their replication and propagation they rely on functions provided in *trans* by their helper viruses. Hence, defective genomes with their simpler structure constitute a convenient system for studying the maturation and cleavage of viral DNA.

In the presence of "foster" helper virus DNA, concatemeric defective genomes can be generated from monomeric seeds (amplicons) containing a replication origin and a cleavage-packaging signal (28). The L-S junctions, as well as the *ba* and *ca* termini, were shown to constitute functional cleavage-packaging signals and to be required for the transmission of replicating amplicons from passage to passage (22–24, 26, 29). Any pair of *a* sequences along the concatemeric molecule could become cleaved, resulting in the packaging of monomers, dimers, and higher multimeric forms of defective genomes into nuclear capsids. However, only full-length (ca. 150-kb) concatemers of defective virus genomes were found to be present in cytoplasmic virions (11, 29).

The *a* sequence contains unique (U) and directly repeated (DR) sequence elements. The *a* sequences of various HSV-1 and HSV-2 strains range in size from 250 to 500 base pairs (bp), depending on the number of reiterations of the DR elements (4, 13, 14). For example, the *a* sequence of HSV-1 (strain F) could be represented by DR1-Ub-$(DR2)_{19}$-$(DR4)_3$-Uc-DR1 (14). The tandemly reiterated *a* sequences present at double *a*-containing (*baac*) junctions were shown to share one DR1 (20-bp) element (i.e., DR1-Ub-$(DR2)_{19}$-$(DR4)_3$-Uc-*DR1*-Ub- $(DR2)_{19}$-$(DR4)_3$-Uc-DR1). The distal DR1 elements in the *ba* and *ca* termini were found to be incomplete and together constituted a DR1 sequence (15). Thus, the *ba* terminus was reported to contain 18.5 bp of the DR1 sequence (i.e., 18 bp and a single-base 3' overhang), whereas the *ac* terminus contained the remaining 1.5 bp. These findings were consistent with the model proposed by Mocarski and Roizman (15), whereby a *baac* junction was cleaved within the shared DR1 sequence to generate the *ba* and *ac* termini. In this respect, the cleavage of viral DNA concatemers presents an enigma in that L-S junctions containing a single *a* sequence are the predominant junctions in concatemeric viral DNA. It is at present unknown whether and how such *bac* junctions can be cleaved to generate the observed ba_n and *ca* ends.

In the present study we have investigated the mechanism of the cleavage-packaging process. Specifically, our studies have shown the following. (i) The cleavage-packaging signal resided within the *a* sequence itself; at least one of the DR1 sequences was not essential for the process. (ii) The cleavage of viral DNA concatemers was coupled to packaging. (iii) *bac*-type junctions could be cleaved into *ba* and *ca*

* Corresponding author.

termini. Therefore, cleavage-packaging occurred by a process involving the amplification of the *a* sequence.

MATERIALS AND METHODS

Cells and virus. The sources for HEp-2 cells, Vero cells, rabbit skin cells, and the HSV-1 strain Justin were described previously (10, 22).

Derivation of plasmids. Cloning was done as previously described (22) with the *Escherichia coli* strains DH1 (gift of D. Hanahan, Cold Spring Harbor Laboratories) and GM48 (1, 12). The structure of plasmids is schematically diagrammed in Fig. 1. The plasmid pRB373 was derived by Macarski and Roizman, and its structure was previously described (16). It contained three segments of HSV-1 (F) DNA including the following: the replication origin, ori-1′ (16, 25, 28), within the *Bam*HI-*Pvu*II segment of the *Bam*HI-N fragment; the *Bgl*II-*Pvu*II segment of *Bam*HI-Q (containing the coding sequences of the thymidine kinase gene); a 1,272-bp L-S junction inserted into the *Eco*RI site of the *Bam*HI-N fragment. The plasmid p-200 was derived from pRB373 by deletion of the 1,272-bp *bac* segment. The plasmid pac-2 was previously described (23) and contained the 1,272-bp L-S junction of pRB373 inserted into the *Eco*RI site of pKC7 (18). The amplicon pF1′-205 was derived by cloning double *a*-containing repeat units of defective genomes present in the virus stocks JRB373. The plasmid was shuttled into bacteria by cleaving the infected cell DNA with *Sal*I (which cleaves once within each monomer), circularizing the resultant monomers by self ligation, and transforming DH1 bacteria. The plasmids pF1′-202, pF1′-211, and pF1′-221 all contained ori-1′ within a *Pvu*II fragment which was taken from p-200. The *Pvu*II ori fragment was introduced into different versions of pac-2 to yield the amplicon pF1′-202, which retained the entire 1,272-bp *bac* sequence; the plasmid pF1′-211 (constructed with an *Sst*II deletion of pac-2), which contained the sequence b-DR1-c; and the plasmid pF1′-221 (constructed with a *Bss*HII deletion of the *a* sequence in pac-2), which contained the sequence *b*-DR1, 28 bp of Ub, 14 bp of Uc, DR1-*c*. The amplicon pF1-241 was constructed in two steps. First, the *Eco*RI-to-*Pvu*II fragment of *Bam*HI-N (containing ori-1′) was inserted between the *Eco*RI and *Pvu*II sites in pBR322. Second, an *Sal*I-*Hin*cII fragment containing the U_S-*a* junction of a HSV-1 (Justin) defective genome repeat unit was taken from pJD101, a cloned repeat unit of the Justin defective genome (13), and was inserted into the *Pvu*II site. The amplicon pF1′-282 contained an isolated *a* sequence and was constructed in three steps. First, pBR322 grown in GM48 (a *dam*$^-$ *dcm*$^-$ strain of *E. coli*) was doubly cleaved with *Bal*I and *Ava*I. The cleaved plasmid was treated with T4 DNA polymerase, followed by the insertion of a *Pst*I linker (GCTGCAGC; New England Biolabs). Second, the 1,272-bp *bac* fragment (purified from pac-2) was fully cleaved with *Xma*III and partially cleaved with *Ava*I. The resultant fragments extended from the *Xma*III site at the *b* border of the *a* sequence to the various *Ava*I sites within the *a* sequence. The mixture of fragments was inserted into the modified pBR322 between the *Xma*III site and the recreated *Ava*I site. Resultant transformants were screened, and one was chosen which contained the *a* sequence from the *Xma*III site at the border between *b* and *a* to the *Ava*I site found in the DR1 sequence at the border between *a* and *c*. Because of the addition of the *Pst*I linker the sequence of the DR1 was exactly restored. This method could produce either an exact copy of DR1 or a copy containing a single base change due to degeneracy of

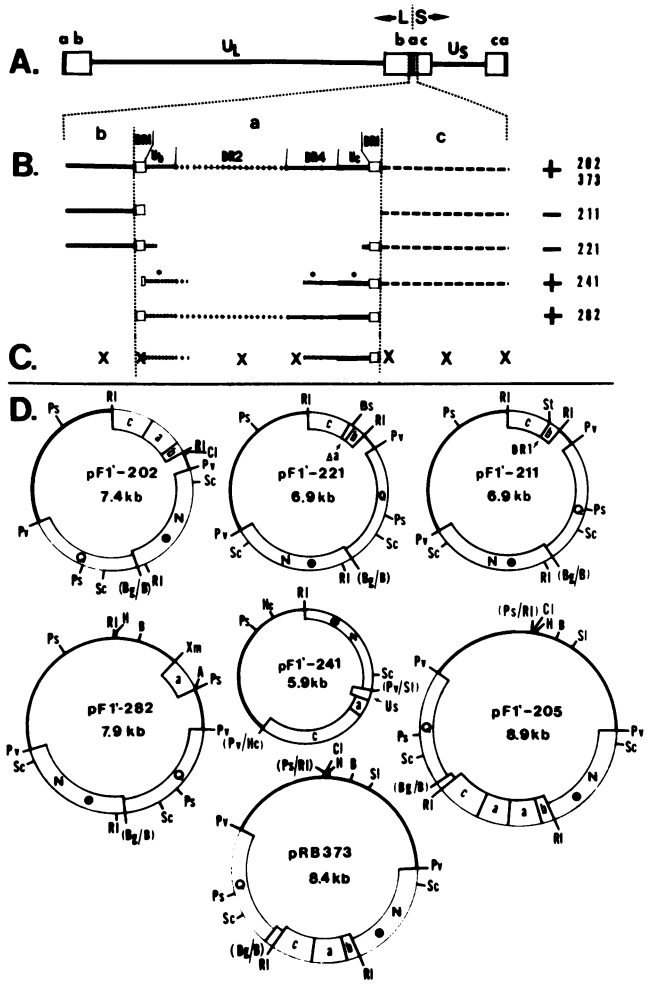

FIG. 1. Structure of test plasmids. A, Structure of standard HSV DNA. B, Expanded representation of an L-S junction containing a single *a* sequence and present in pRB373, derived by Mocarski and Roizman (16) and in pF1′-202. The organization of the directly repeated (DR) and unique (U) elements are for the HSV-1 F strain, as shown by Mocarski and Roizman (14). Subsets of the *bac* sequences present in the various test plasmids are shown. Asterisks in pF1′-241 denote sequence elements contained in the *a* sequence of the Justin defective genome cloned repeat unit. The Uc, DR2, DR4, and Ub elements in this *a* sequence are closely related in the Justin and F strains (13). The + and − symbols denote the ability of the test construct to propagate as defective virus genomes in serially passaged virus stocks. C, Summary of the amplicon propagation tests. Regions not essential for propagation are marked with X. D, Schematic representation of the test plasmids. Bacterial plasmid DNA sequences are denoted by heavy lines. HSV DNA inserts are denoted by double lines. Q and N refer to subsets of the *Bam*HI Q and N fragments of HSV-1 (F) DNA. The filled circle in *Bam*HI-N denotes the replication origin ori-1′. Shown are the sites for *Ava*I (A), *Bam*HI (B), *Bss*HII (Bs), *Bgl*II (Bg), *Cla*I (Cl), *Hin*dIII (H), *Hin*cII (Hc), *Pst*I (Ps), *Pvu*II (Pv), *Eco*RI (RI), *Sac*I (Sc), *Sal*I (Sl), *Sst*II (St), and *Xma*III (Xm). Bg/B, Ps/RI, Pv/Sl, and Pv/Hc denote the fusion of the respective sites. Δa in pF1′-221 denotes the remaining portions of the *a* sequence after deletion of the internal *Bss*HII fragment. Us denotes 174 bp of U_S sequences present in the cloned Justin defective genome repeat. These sequences are fused to the *a* sequence at the DR1 element (13).

the *Ava*I recognition sequence (CPyCGPuG). We chose the exactly repaired DR1 sequence. Finally, the ori-1′ *Pvu*II segment (from p-200) was inserted into the *Pvu*II site of the *a*-containing plasmid, yielding the pF1′-282 amplicon. pF1′-282 thus contains a complete *a* sequence flanked by plasmid DNA on both sides with no remaining *b* or *c* sequences.

Cotransfection of cells and passaging of virus stocks. Cotransfection of cells with helper virus DNA and test amplicons was done as previously described (22) with 0.5 μg of test plasmid DNA, 1 μg of helper virus DNA, and 5 μg of salmon sperm carrier DNA per 25-cm^2 rabbit skin cell culture. Virus harvested from the transfected culture was designated as PO. Virus was propagated in HEp-2 cells at a 1:4 dilution. The virus series derived from the cotransfections were designated with the first letter of the helper virus followed by the amplicon designation (e.g., JRB373 refers to a virus series produced from a cotransfection receiving the helper HSV-1 [Justin] DNA and the amplicon pRB373).

Analyses of total infected cell DNA. Virally infected cells were treated with sodium dodecyl sulfate-proteinase K followed by phenol-chloroform extraction and ethanol precipitation of total nucleic acids (11). Cells were labeled with $^{32}P_i$ as previously described (22). Restriction enzymes, T4 DNA ligase, and T4 DNA polymerase were purchased from Bethesda Research Laboratories or New England Biolabs and used as suggested by the vendor. λ-Exonuclease was purchased from New England Biolabs and used as previously described (10). Southern blot hybridizations were done essentially as described by Southern (21), except that the transfers were performed in 20× SSC (1× SSC is 0.15 M NaCl plus 0.015 M sodium citrate).

Preparation of cytoplasmic and nuclear DNase-protected DNA. DNase-protected DNA was prepared from the cytoplasmic and nuclear fractions of infected cells as previously described (6, 28). Briefly, the nuclear and cytoplasmic fractions of infected cells were obtained by Nonidet P-40 lysis and were divided into two equal samples, one of which was treated with deoxycholate and DNase I (50 μg/ml, 10 min, 37°C) followed by proteinase K-sodium dodecyl sulfate digestion, extraction with phenol and chloroform–2% isoamyl alcohol, and ethanol precipitation. The other sample was similarly treated, except that the DNase I was omitted.

RESULTS

Mapping of the cleavage-packaging signal. In the studies described below we have employed the transfection-propagation assays for HSV amplicons (22, 28) to map the cleavage-packaging signal. Specifically, amplicons containing modified L-S junctions in addition to a functional replication origin (ori-1′) were used to cotransfect cells in the presence of helper virus DNA. The transfection derived virus stocks were further propagated through several serial passages and analyzed for the presence of generated defective genomes. Only defective genomes arising from seed plasmids containing a functional cleavage-packaging signal are expected to be recovered in transfection-derived virus stocks after serial propagation (23, 26). These analyses therefore provided a test for the presence of a functional cleavage-packaging signal within the constructed plasmids. In addition, the structure of termini generated from altered cleavage substrates could be determined.

The construct pRB373 (Fig. 1) served as the starting test plasmid. This plasmid was derived by Mocarski and Roizman (16) in the course of their study of sequences involved in the S-L inversions. It contained three sets of HSV-1 (F)

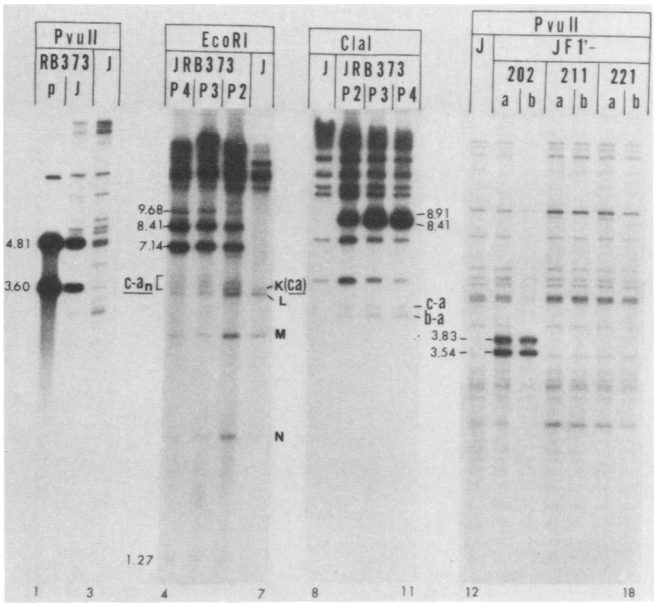

FIG. 2. Tests for propagation of constructed plasmids in transfection derived virus stocks. Lane 1 shows *Pvu*II-digested, ^{32}P-labeled pRB373 plasmid DNA serving as size marker. Lanes 2 through 18 show restriction enzyme digests of ^{32}P-labeled total DNA from cells infected with standard helper virus control (designated J, lanes 3, 7, 8, and 12), or infected with the second, third, and fourth passages (P2, P3, and P4) of a series generated from a cotransfection receiving the pRB373 amplicon (lanes 2, 4, 5, 6, 9, 10, and 11), or infected with the second passages of duplicate series (a, b) derived from independent cotransfections with HSV-1 (Justin) helper virus DNA and the test plasmids pF1′-202, pF1′-211, and pF1′-221. *ca* and *ba* denote fragments representing the termini of the generated defective virus genomes. Underlined *c*-a_n denotes the series of bands (containing variable numbers of *a* sequences) derived from the S terminus of the helper virus genomes in the serially passaged virus stocks. Numbers denote fragment sizes in kilobases. The 8.41- and 9.68-kb bands represent partial *Eco*RI cleavage products.

DNA sequences: (i) a segment of the *Bam*HI-Q fragment, containing the *tk* gene (this segment was present in the original construct and is not directly relevant to the studies described in the present paper); (ii) a segment of the *Bam*HI-N fragment containing the S replication origin, ori-1′; and (iii) a 1,272-bp *bac* (L-S) junction containing a functional cleavage-packaging signal. This junction consisted of 156 bp of *b* sequences, the 501-bp *a* sequence, and 615 bp of *c* sequences (16).

To test for the ability of the pBR373 amplicon to replicate and become propagated within virions in virus stocks, cells were cotransfected with the pRB373 plasmid and helper virus DNA. Virus derived from these cotransfections was serially propagated, and ^{32}P-labeled DNA prepared from cells infected with passages 2 through 4 of the resultant series was digested with restriction enzymes and analyzed in gels. The Justin strain of HSV-1 was chosen as the helper virus because it contained a 244-bp *a* sequence (10, 13) distinct from that present in the pRB373 amplicon (501 bp [14]). It was thus possible to determine whether an *a* sequence appearing in defective genomes indeed originated from the *a* sequence in the test amplicon or arose (by recombination) from the helper virus DNA.

Comparison of *Pvu*II digests of ^{32}P-labeled helper virus DNA (Fig. 2, lane 3), with the *Pvu*II digests of ^{32}P-labeled DNA from cells infected with passage 4 of the transfection-

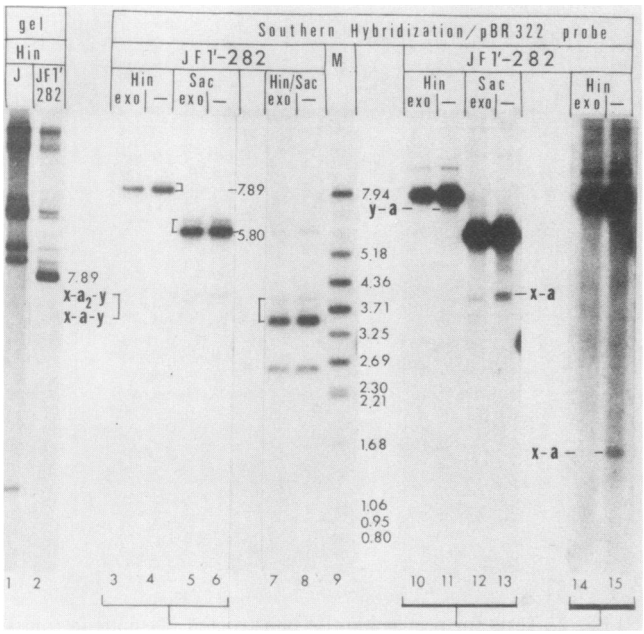

FIG. 3. Structural analyses of defective genomes propagated from the pF1'-282 amplicon. Lanes 1 and 2 show *Hin*dIII digests of ^{32}P-labeled DNA from cells infected with standard Justin virus and passage 2 of the JF1'-282 series. Lanes 3 through 8 show hybridization of ^{32}P-labeled pBR322 probe to Southern blots containing *Hin*dIII- (Hin), *Sac*I- (Sac), and *Hin*dIII-SacI-cleaved unlabeled passage 2 DNA of the JF1'-282 series. Cleavage was done either directly (−) or after λ exonuclease digestion. To more clearly show the terminal bands, *x-a* and *y-a*, lanes 10 through 13 show longer autoradiographic exposures of lanes 3 through 6, and lanes 14 and 15 show even longer exposures of lanes 3 and 4, respectively. *x-a-y* and *x-a*$_2$*-y* denote the fragments containing the single *a* and double *a* junctions. The solid line connecting the two bands in lanes 3 through 8 denotes the multiple *a* increment.

derived virus (lane 2) revealed the presence of defective genomes consisting predominantly of 8.41-kb repeat units, which were identical to the seed pRB373 plasmid (lane 1). On the basis of these results and in accordance with previous results (23), we conclude that the *bac* junction in the pRB373 construct contained a functional cleavage-packaging signal. Lanes 4 through 11 of Fig. 2 show the *Eco*RI and *Cla*I digestion patterns of the helper and defective virus DNAs and are further discussed below in sections concerning the structure of the generated termini.

To map the cleavage-packaging site, we tested the ability of plasmids containing altered *bac* junctions to propagate in virus stocks. The test plasmids (Fig. 1) included the following: (i) pF1'-202, which contained the unaltered *bac* sequence and served as a positive control; (ii) pF1'-211, which contained the *b* and *c* sequences flanking a DR1 sequence; (iii) pF1'-221, which contained the *b* and *c* sequences flanking a *Bss*HII-deleted *a* sequence (the deleted *a* consisted of the sequence DR1-Ub(28 bp)-Uc(14 bp)-DR1); (iv) pF1'-282, which contained an intact *a* sequence, with bacterial plasmid DNA replacing the flanking *b* and *c* sequences. Each of these plasmids was tested for the ability to propagate as defective genomes in two separate cotransfection tests (a and b). The transfection-derived stocks were passaged, and ^{32}P-labeled DNAs from cells infected with passages 2 through 4 were analyzed with restriction enzymes. The results of these analyses revealed that both the *bac* control plasmid (pF1'-202) and the construct containing the intact *a* sequence without *b* or *c* flanking sequences (pF1'-282) were efficiently propagated (Fig. 2, lanes 12 through 18; Fig. 3, lanes 1 and 2). In contrast, the plasmids containing *b*-DR1-*c* (pF1'-211) and the *Bss*HII-deleted *a* sequence (pF1'-221) were not efficiently propagated in serially passaged virus stocks. These results were further confirmed by Southern blot hybridizations with pBR322 as a probe (Fig. 3, lanes 3 through 15, and data not shown). Taken together these studies revealed that the *a* sequence itself contained a functional cleavage-packaging signal, that the *b* or *c* sequences were not required, and that internal regions of the *a* sequence formed a necessary part of this signal.

Role of the DR1 sequence in the cleavage-packaging process. Defective genomes accumulating in serially passaged HSV-1 (Justin) stocks are composed of 8.4- to 8.6-kb repeat units, corresponding to the entire *ac* inverted repeat sequence of S, and the adjacent U_S sequence (11). Nucleotide sequencing of a cloned defective genome repeat unit revealed that within the concatemeric defective virus DNA the U_S sequences of one repeat were directly joined to the *a* sequence of the adjacent repeat, forming a novel (U_S-*a*) junction between adjacent repeats. The transition from U_S to *a* sequences occurred within the DR1 element, leaving only 4 bp of the 20-bp element (13). The *a* sequence in the cloned defective genome repeat therefore contained an intact DR1 sequence on the *c* side, but only 4 bp of DR1 on the U_S (equivalent to the *b*) side.

To investigate the role of DR1 elements in the cleavage-packaging process we constructed the amplicon pF1'-241, which contains the U_S-a junction. This amplicon was employed in two series of cotransfections using as helper viruses either the HSV-1 Justin strain, which contains a 264-bp *a* sequence, or HSV-1 strain F, which contains a 501-bp *a* sequence. These two helper viruses were chosen to allow unambiguous identification of *a* sequences recovered within the propagated defective genomes. The resultant series (JF1'-241 containing the Justin helper virus and FF1'-241 containing the F helper virus) were propagated as described above, and ^{32}P-labeled DNA prepared from cells infected with passage 2 virus was analyzed by restriction enzymes. The results of these analyses (Fig. 4, lanes 1 through 7, and data not shown) revealed that the pF1'-241 amplicon was successfully propagated. Southern blot hybridization analyses were also done (Fig. 4, lanes 8 through 16). As discussed below, these analyses revealed that the *a* sequence found within the generated defective genomes originated from the seed repeat rather than the helper virus DNA. On the basis of these data we conclude that the complete DR1 sequence did not form an essential part of the cleavage-packaging signal.

Structure of the junctions and termini in JRB373 defective genomes. Using the constructed defective virus genomes described above, we next examined the structural features of the junctions between adjacent repeat units and the termini generated by cleavage of these junctions. As an example, we shall first describe the analyses of viral genomes present in the series JRB373 (derived from a cotransfection receiving the pRB373 amplicon and the Justin helper virus DNA). (i) ^{32}P-labeled JRB373 DNA was digested with restriction enzymes. (ii) Southern blot hybridizations were done with four probes: *Bam*HI-Q, *Bam*HI-N, the *bac* sequence itself, and pBR322. Each of these probes was expected to hybridize to a different set of fragments in the digested DNA and to highlight the features of one or the other termini. For example, after *Sac*I cleavage, the *Bam*HI-N probe will

hybridize to the *ba* terminus, and the *Bam*HI-Q probe will hybridize to the *ca* terminus (Fig. 1). (iii) A sample of the DNA was treated with λ exonuclease before restriction enzyme digestion and blotting to allow unambiguous identification of the terminal fragments. Thus, terminal fragments were identified on the basis of size, hybridization with specific probes, and sensitivity to λ exonuclease digestion. HSV-1 (Justin) DNA extracted from cells infected with standard virus (J) was similarly analyzed to identify the bands arising by digestion of the helper virus DNA.

The results of these analyses revealed the following. (i) As expected, standard virus DNA molecules contained a variable number of *a* sequences at the L-S junctions and the L termini (e.g., the underlined ba_nc and ba_n bands in Fig. 5, lanes 1 and 4). (ii) The majority of junctions in the constructed defective genomes corresponded to the input *bac*-type junctions. However, a minor proportion of the junctions contained two copies of the *a* sequence (band labeled 8.91 in Fig. 2, lanes 9 to 11; bands labeled ba_2c in Fig. 5, lanes 3, 7, and 13, and in Fig. 6, lanes 9 and 10). As judged from the increment between the *baac* and *bac* bands (ca. 500 bp), the amplified *a* sequences originated from the input amplicon rather than from the Justin helper DNA (*a* is 264 bp). Hence, the signal for *a* amplification resided within the *bac* sequences contained in the pRB373 amplicon. (iii) The defective genome termini were predominantly *ba* and *ca* (bands labeled *ba* and *ca* without underline Fig. 2, lanes 9 to 11, and Fig. 5, lanes 6, 7, 8, 15, and 16), although longer gel exposures and additional cleavages (Fig. 6, lanes 5 and 6, and additional data not shown) revealed a small fraction of *baa* termini. We have not detected significant proportions of λ exonuclease-sensitive termini devoid of *a* sequences (i.e., *b* or *c* termini). (iv) Despite the qualitative resemblance, amplified *a* sequences in the junctions and termini of the defective genomes were less prevalent than in their standard virus counterparts. For example compare the ratios of the different bands in the ba_nc and ba_n families in Fig. 5, lanes 1 and 4 (standard) and lanes 3, 6, and 7 (defective genomes). (v) Alterations were noted in the structure of the S termini of the helper virus DNA molecules which were present in the serially passaged virus stocks, indicating that the abundant presence of defective genomes interfered with the normal maturation processes of the helper virus DNA. Specifically, significant proportions of the standard virus DNA molecules in the defective virus stocks appeared to terminate with *caa* and *caaa* sequences in addition to the standard *ca* S end (underlined ca_2, ca_3 bands in Fig. 5, lane 6). Interestingly, long autoradiographic exposures of the hybridized blots revealed the presence of *caa* and *caaa* termini in standard virus DNA molecules (propagated in the absence of defective virus genomes), albeit at substantially lower proportions (underlined ca_2, and ca_3 bands in Fig. 5, lane 4). The simplest explanation to these observations was that the aberrent S termini represented unstable intermediates in a normal maturation process of standard virus DNA, and that this process was interfered with by excess defective genomes, resulting in increased proportions of the ca_2 and ca_3 bands. Further support for this hypothesis came from the restriction enzyme patterns of ^{32}P-labeled DNAs of passages 2 through 4 of the JBR373 series, where the relative abundance of S ends containing *a* reiterations appeared to increase in relation to the proportion of defective genomes (Fig. 2, lanes 4 through 7).

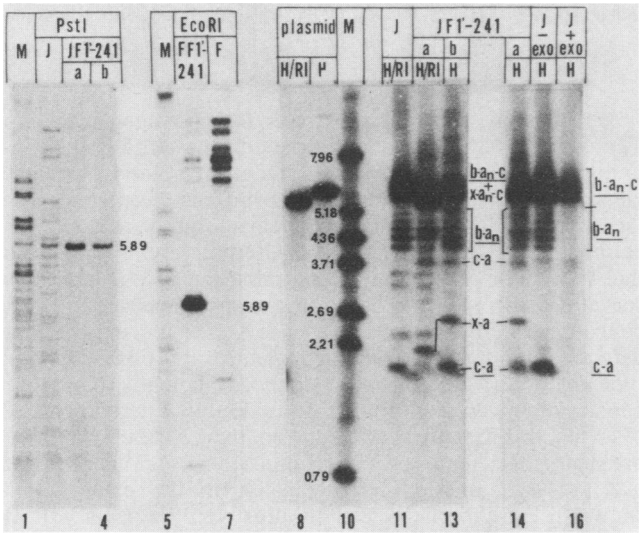

FIG. 4. Propagation of the pF1'-241 amplicon. Lanes 1 through 7 show restriction enzyme analyses of ^{32}P-labeled DNA from cells infected with standard HSV-1 strains Justin (lane 2) and F (lane 7) or infected with the second passages of two independently derived JF1'-241 series (lanes 3 and 4) and passage 2 of the series FF1'-241 (lane 6). An *Sal*I digest of HSV-1 (Justin) DNA was included (lanes 1 and 5) as a size marker. Lanes 8 through 16 show Southern blot hybridizations with ^{32}P-labeled *a* probe purified from pF1'-282. The blots contained the seed plasmid pF1'-241 cleaved with *Hin*cII (H) or *Hin*cII-*Eco*RI (H/RI) (lanes 8 and 9) and digested DNA from cells infected with the Justin helper virus (lanes 11, 15, and 16) or infected with passage 2 of the two independantly derived JF1'-241 series (lanes 12 through 14). Lane 10 contained a mixture of fragments, serving as size markers. The identification of the terminal helper virus DNA fragments was confirmed by their sensitivity to λ exonuclease (lane 16 compared with lane 15). The L-S junctions and termini of the helper virus DNA are underlined.

Analyses of junctions and termini in additional constructed defective genomes. In describing the remaining constructed virus populations it is convenient to designate the various junctions present in the HSV amplicons as *xay* where *x* and *y* represent the sequences flanking *a*. In pF1'-202 *x* and *y* correspond to *b* and *c*, respectively, in pF1'-282 they correspond to bacterial plasmid sequences and in pF1'-241 they correspond to the U_S and *c* sequences, respectively. Restriction enzyme analyses and Southern blot hybridizations of DNA in these series (Fig. 3 and 4 and data not shown) yielded results similar to those described for the JRB373 passaged virus. (i) Mainly all of these constructs yielded defective virus genomes with predominantly single *a* (input-type) junctions. However, without exception, all of the generated virus stocks also contained minor proportions of repeat units with multiple *a*-containing junctions (e.g., band labeled $x\text{-}a_2\text{-}y$ in Fig. 3, lanes 3 to 8). In all cases the amplified *a* sequences were derived from input amplicon rather than from helper virus DNA. (ii) Defective genomes arising by propagation of amplicons with *xay* junctions contained predominantly *xa* and *ya* termini (bands labeled *x-a* and *y-a* in Fig. 3, lanes 10 to 15, and bands labeled *c-a* and *x-a* in Fig. 4, lanes 12 to 14). Termini (sensitive to λ exonuclease) devoid of *a* sequences were not detected.

Analyses of defective genomes generated from a double *a*-containing amplicon. The finding of *xa* and *ya* termini in defective virus genomes containing predominantly *xay* junctions prompted us to examine in detail the structure of defective genomes evolving from double *a* containing amplicons. Specifically, a repeat unit containing a *baac* junction was shuttled from the JRB373-infected cells into

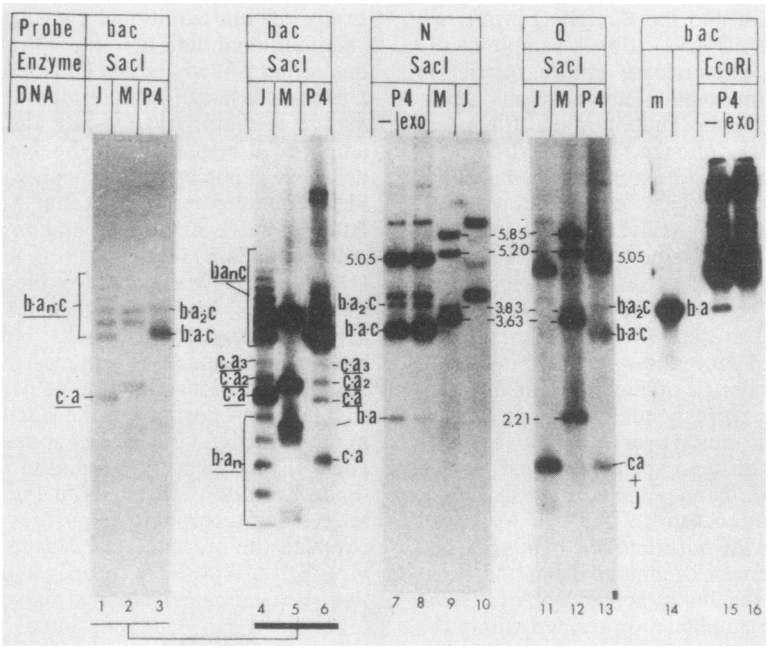

FIG. 5. Southern hybridization of pRB373-derived defective genomes. Unlabeled DNA prepared from cells infected with standard virus (J) or passage 4 of the JRB373 series (P4) was digested with *Sac*I or *Eco*RI either directly (−) or after digestion with λ exonuclease (exo). The separated fragments were transferred to nitrocellulose strips and hybridized with ^{32}P-labeled probes including the plasmids pRB103 (containing *Bam*HI-Q), and p-ori-1 (carrying the ori-1′-containing *Eco*RI-*Pvu*II segment of *Bam*HI-N), and a gel-purified 1,272-bp *bac* fragment obtained by digestion of pRB373 with *Eco*RI. M (lanes 2, 5, 9, and 12) denotes a mixture of restriction enzyme fragments serving as size markers. m (lane 14) represents a 657-bp fragment serving as a marker for the expected 657-bp *ba* terminus. Lanes 4 through 6 are longer autoradiographic exposures of lanes 1 through 3. The junctions and termini of the helper virus DNA are underlined. Junctions and termini from the generated defective genomes are not underlined.

bacteria. The resultant plasmid, pF1′-205 (Fig. 1), was then used as a seed amplicon in a new set of cotransfections with the Justin helper virus DNA. Comparison of the pF1′-205 (double *a*) derived defective genomes with those derived from pRB373 (single *a*) revealed the following. (i) Significant proportions of the pF1′-205-derived defective genomes carried single *a* junctions, despite the fact that the input amplicon contained a *baac*-type junction. Nonetheless, considerably higher proportions of double *a* junctions were present in these defective genomes than in those derived from the pRB373 amplicon. For example, compare the relative intensities of the bands designated *bac* and ba_2c in Fig. 6, lanes 10 (single *a* amplicon) and 11 (double *a* amplicon). (ii) The increase in abundance of the double *a*-containing junctions in JF1′-205 was paralleled by increased relative abundance of the *baa*-type terminus (compare the ratio of *ba* and ba_2 bands in lanes 5 and 8, Fig. 6). (iii) Two additional bands hybridizing to the pBR322 probe were present in the pF1′-205-derived stocks (bands I and II in Fig. 6, lane 8). The nature of DNA contained in these bands is currently unknown, although the same bands were reproducibly observed in an additional virus stock that was independently derived from pF1′-205 (data not shown). Furthermore, similar bands were present in the pRB373 derived virus, albeit at reduced relative amounts (Fig. 6, lane 5). These bands may therefore represent intermediates in the maturation-cleavage of the defective genomes. Both bands were found to be resistant to λ exonuclease digestion (data not shown) and may represent either internal sequences or terminal structures resistant to the λ exonucleolytic attack. Further analyses of the structure of these bands are underway.

***bac* junctions serve as substrates for cleavage-packaging.** The constructed defective genomes discussed thus far contained predominantly *xay* junctions and *xa* and *ya* termini. Generation of *xa* and *ya* termini during the cleavage of *xay* junctions would imply that the cleavage process itself was coupled to the amplification of *a*. Alternatively, it is possible that the minor repeat units containing multiple *a* junctions served as the sole target for the cleavage of viral DNA concatemers. If this were the case we would expect that defective genomes containing higher proportions of *baac* type junctions would be packaged more efficiently than those containing lower proportions of the double *a* junctions.

To test this hypothesis we have compared the efficiency of packaging of defective genomes containing various ratios of *bac* to *baac* junctions. Specifically, in the experiments shown in Fig. 7 replicate cell cultures were infected with (i) standard HSV-1 (Justin) alone, (ii) P1 of the series JF1′-202 (derived from the single *a*-containing amplicon), (iii) P2 of the series JF1′-205 (derived from the double *a*-containing amplicon), and (iv) a 1:1 mixture of the two series above. As judged by densitometric scanning of gel autoradiograms, defective genomes present in these passages of the JF1′-202 and JF1′-205 series contained 2 and 35% *baac*-type junctions, respectively.

The efficiency of packaging was determined by analyzing the relative amounts of the various DNA species (helper and the two types of defective genome repeats) in the nuclear or cytoplasmic fractions before and after digestion with DNase. In these experiments infected cells were separated into nuclear and cytoplasmic fractions. Half of each fraction was treated with DNase I to digest free (nonencapsidated) DNA (6, 28), and DNAs prepared from the four fractions were

digested with a number of restriction enzymes. We then compared the relative ratio of bands representing the helper virus DNA and the two types of defective genomes in the total and DNase-protected nuclear and cytoplasmic DNA fractions. The results of these analyses (Fig. 7 and data not shown) revealed the following. (i) DNase digestion of the nuclear fraction resulted in efficient degradation of free (nonencapsidated) DNA as clearly demonstrated by the selective elimination of host DNA after the DNase treatment. This can best be seen by comparing the amount of *Sal*I-resistant host DNA in the various fractions (see legend to Fig. 7, lanes 1 to 16). (ii) The abundance of standard virus genomes relative to defective genomes remained unchanged through the various fractionation protocols. (iii) Similarly, analyses of DNase-protected DNA from the mixed infected culture (JF1′-202 plus JF1′-205) revealed that the relative ratio of defective genomes containing *bac* or *baac* junctions remained constant through the different fractionation protocols. Taken together, these observations revealed that defective virus DNA molecules containing single *a* and double *a* junctions were packaged with equivalent efficiency and that both were packaged as efficiently as the standard virus DNA. (iv) Fragments representing the defective genome termini were underrepresented in the total nuclear DNA. (Fig. 7; compare the ratio of *ba* and *ca* fragments to the internal 8.41- and 8.91-kb fragments in the total [lane 27] and DNase-protected [lane 28] nuclear fractions.) This result reflected the nuclear presence of substantial proportions of DNA molecules within "endless" concatemers, as previously reported for standard virus DNA (7). (v) To allow visual comparison of the relative ratios between the various bands, we have included in Fig. 7 shorter autoradiographic exposures of the lanes containing total nuclear DNA samples. The total nuclear fraction contained significantly higher amounts of total DNA and would show as very dark lanes on exposures for the same length of time as that required to clearly show the other fractionated DNA samples. When the autoradiographic exposures of equivalent length (data not shown) of the lanes containing nuclear encapsidated and total nuclear DNA were compared, the amounts of the *ba* and *ca* fragments in the total nuclear fraction were similar to those in the DNase-protected fraction. These results revealed that the majority of the *ba* and *ca* termini present in the total nuclear fraction were in fact contributed by packaged DNA. This last observation provided further support to the conclusion that the generation of termini was coupled to packaging, such that only packaged DNA (DNase protected) contained the cleaved termini.

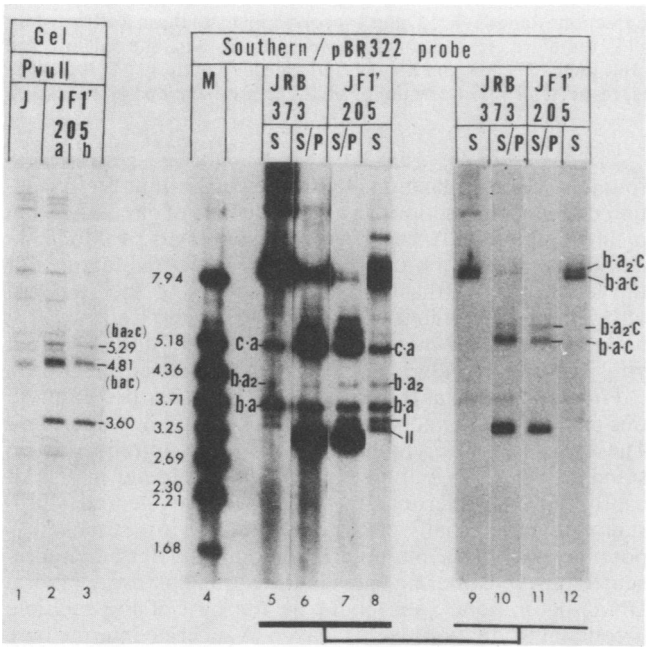

FIG. 6. Characterization of virus stocks derived from single *a*-containing (pRB373) and double *a*-containing (pF1′-205) amplicons. Lanes 1 through 3 show *Pvu*II-digested, ^{32}P-labeled DNA from cells infected with standard HSV-1 (Justin) and from cells infected with passage 2 of two independently derived JF1′-205 series. Lanes 4 through 8 show Southern blot hybridizations with a pBR322 probe. The blot contained *Sal*I-digested (S) and *Sal*I-*Pst*I-digested (S/P) DNA from cells infected with passage 5 of the JRB373 series or digested DNA from cells infected with passage 2 of the JF1′-205 series. Lanes 9 through 12 show a shorter autoradiographic exposure of lanes 5 through 8. The defective virus termini and junction fragments are marked. The bands marked I and II, which appear in higher proportions in the stock derived from the double *a* amplicon (compare lanes 5 and 8), are discussed in the text.

DISCUSSION

Viral DNA replication in HSV-infected cells was shown to involve the formation of large concatemeric DNA molecules containing head-to-tail reiterations of the 150-kb viral genome. In the work reported above we have employed constructed HSV defective genomes to study the cleavage and packaging of large concatemeric viral DNA. Four major conclusions can be drawn from this work.

First, the signal specifying the cleavage-packaging of viral DNA was mapped within a 248-bp *a* sequence derived from a cloned HSV defective genome. This finding was significant in that the *a* sequence in this clone contained only 4 bp of the 20-bp DR1 element, which was previously shown to become cleaved during the generation of the S terminus of mature standard virus DNA (13, 15). This result provided further support for our previous hypothesis that the cleavage-packaging process involved the recognition of sequences at internal locations within the *a* sequence, rather than the recognition of the DR1 sequence itself (13). Cleavage could thus involve a measuring function to defined distances away from the internal recognition signal. Indeed, as our studies further show, the deletion of internal *a* sequences, including the well-conserved regions of Ub and Uc, abolished the ability of amplicons to propagate in serially passaged virus stocks. In this respect it is noteworthy that at the time of submission of this manuscript Varmuza and Smiley reported similar conclusions on the basis of insertions of modified *a* sequences into internal locations (*tk*) of the standard virus DNA (27).

A second conclusion from the studies reported in this paper was that the cleavage of viral DNA concatemers was linked to the packaging process itself. Our studies have shown that the majority, if not all, of the molecules with *ba* and *ca* termini were present within DNase-protected structures in the nuclei of the infected cells. These quantitative analyses have extended our previous results concerning defective virus genomes, as well as the results of genetic studies by Ben-Porat and co-workers concerning the cleavage and packaging of pseudorabies virus DNA (8, 9).

Third, the results reported above strongly suggest that the cleavage-packaging process is accompanied by the amplification of an *a* sequence. Several observations support this claim, specifically, (i) the finding that constructed defective genomes containing predominantly *xay* type junctions carry

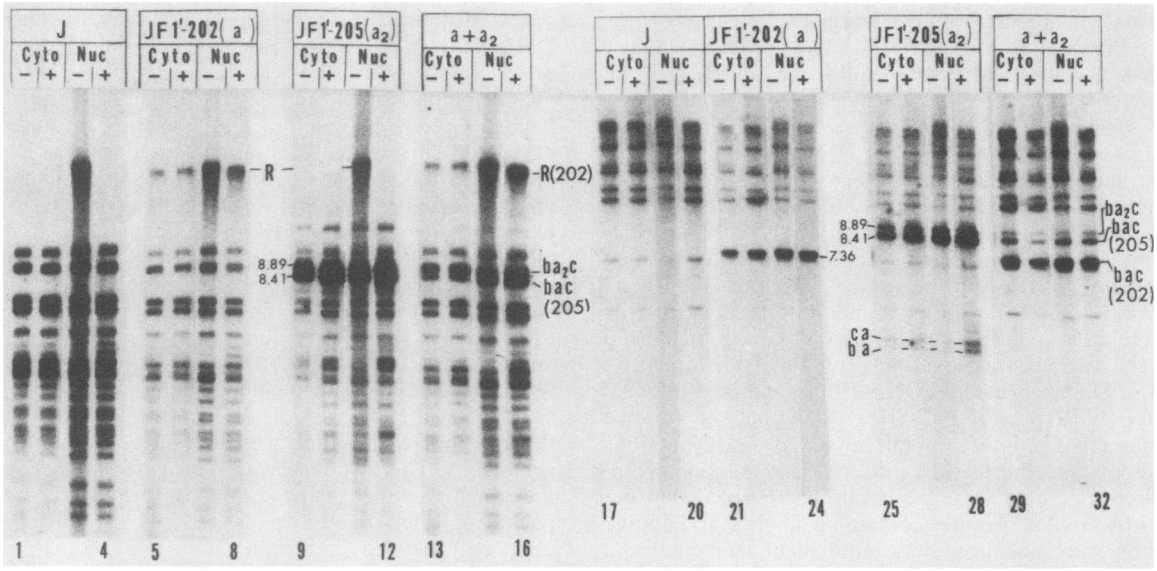

FIG. 7. Packaging efficiency of single and double *a*-containing defective virus genomes. ^{32}P-labeled cells infected with the indicated viral stocks were fractionated as described in Materials and Methods. Equal samples of the cytoplasmic (Cyto) and nuclear (Nuc) extracts were either digested (+) or were not digested (−) with DNase before proteinase K-sodium dodecyl sulfate treatment and DNA purification. Lanes 1 through 16 show *Sal*I digestion patterns demonstrating the effectiveness of DNase digestion. Host DNA present in the total nuclear fraction (e.g., lane 3) was relatively resistant to the *Sal*I enzyme and migrated predominantly as a heterogeneous high-molecular-weight band (R) at the top of 0.5% agarose gels. The high-molecular-weight band was absent from the cytoplasmic fractions and from the DNase-digested nuclear fraction (lanes 1, 2, and 4), thus revealing the efficient removal of nonencapsidated DNA molecules. The pF1′-202 construct does not contain any *Sal*I sites and therefore gives rise to defective genomes which are resistant to *Sal*I. The material migrating as *Sal*I-resistant DNA in the DNase-treated nuclear fraction (lanes 8 and 16) as well as both cytoplasmic fractions (lanes 5, 6, 13, and 14) corresponds to these *Sal*I-resistant defective genomes. The plasmid pF1′-205 contained a single *Sal*I site and is therefore cleaved to a monomer; in this case the single *a* and double *a* repeats are clearly seen (denoted *bac* and ba_2c in lanes 9 through 16). Lanes 17 through 32 show *Cla*I digestion patterns. *Cla*I cleaves both pF1′-202 and pF1′-205 once, yielding 7.36- and an 8.89-kb fragments, respectively. The termini of pF1′-205 are indicated as *ba* and *ca* (lanes 25 through 28).

predominantly *xa* and *ya* termini, (ii) the finding that increased abundance of *baac* junctions was correlated with increased proportions of *baa* ends, (iii) the finding that *bac*-containing defective genomes were packaged as efficiently as their *baac*-containing counterparts, and (iv) the finding that all single *a*-containing amplicons which contained a functional cleavage-packaging signal gave rise to defective genomes containing minor but measurable proportions of double *a* junctions. Taken together these observations strongly suggest that the signal for *a* amplification resides within the *a* sequence itself and that the cleavage-packaging process ultimately produces two *a*-containing termini from single *a*-containing junctions.

Although the details of processes involved in the *a* amplification have yet to be elucidated, there are at least two mechanisms which appear to lead to the *a* amplification. By one mechanism, cleavage-packaging may constitute a two-step process including (i) the amplification of an *a* sequence within the junction to be cleaved and (ii) the subsequent cleavage of the amplified junction, through the splitting of a shared DR1 element (or other sequence located at a constant distance from the internal cleavage signal). Conceivably, this process would result in internal *a* amplification if some of the amplified junctions were to escape the cleavage step. The second mechanism which most likely leads to *a* amplification involves the formation of the *baac* junctions through the circularization of viral DNA. By this mechanism, the *baac* junctions could evolve from *bac* junctions through (i) cleavage (of *bac*) occurring during one round of viral replication, yielding *ba* and *ca* termini, and (ii) formation of the double *a* junction during circularization of the viral DNA in the next round of virus replication. It is noteworthy that the formation of double *a* junctions as a consequence of circularization of input virus DNA was originally suggested by Mocarski and Roizman (15), on the basis of the structural features of the junctions and the terminal sequences of the standard virus genome. Furthermore, Poffenberger and Roizman (17) have recently shown that significant proportions of input viral genomes circularize during initial stages of infection.

Finally, an unexpected result of the studies presented in this paper was the finding of multiple *a*-containing S termini. These species were found to be present infrequently in standard virus DNA; however, they were found in significantly higher proportions in the helper virus genomes present within the serially passaged defective virus stocks. It is possible that these multiple *a*-containing S termini represented unstable intermediates in the normal pathway of viral DNA maturation. Such could be the case if the multiple *a*-containing junctions were cleaved to generate intermediate S termini containing multiple copies of *a*, which would be further processed to generate the observed *ca* termini. The increased abundance of these species in the serially passaged virus stocks could be due to competition for limited machinery needed for the full maturation of viral DNA. Studies designed to investigate the role of such aberrantly processed termini are currently underway.

ACKNOWLEDGMENTS

We thank B. Roizman and E. Mocarski for the gift of pRB373 and pRB103. We thank G. McCray for her technical help.

These studies were supported by Public Health Service research grants AI-15488 and CA-19264 from the National Cancer Institute,

and by National Science Foundation Grant PCM 8118303. L.P.D. is a predoctoral trainee supported by Public Health Service training grant CA-09241 from the National Institutes of Health.

LITERATURE CITED

1. **Backman, K.** 1980. A cautionary note on the use of certain restriction endonucleases with methylated substrates. Gene **11**:169.
2. **Ben-Porat, T.** 1982. Organization and replication of herpesvirus DNA, p. 147–172. *In* A. S. Kaplan (ed.), Organization and replication of Viral DNA. CRC Press, Boca Raton, Fl.
3. **Ben-Porat, T., and S. A. Tokazewski.** 1977. Replication of herpesvirus DNA. II. Sedimentation characteristics of newly-synthesized DNA. Virology **79**:292–301.
4. **Davison, A. J., and N. M. Wilkie.** 1981. Nucleotide sequences of the joint between the L and S segments of herpes simplex virus type 1 and 2. J. Gen. Virol. **55**:315–331.
5. **Frenkel, N.** 1981. Defective interfering herpesviruses, p. 91–120. *In* A. J. Nahmias, W. R. Dowdle, and R. S. Schinazi (ed.), The human herpesviruses—an interdisciplinary prospective. Elsevier/North Holland Publishing Co., New York.
6. **Gibson, W., and B. Roizman.** 1972. Proteins specified by herpes simplex virus. VIII. Characterization and composition of multiple capsid forms of subtypes 1 and 2. J. Virol. **10**:1044–1052.
7. **Jacob, R. J., L. S. Morse, and B. Roizman.** 1979. Anatomy of herpes simplex virus DNA. XII. Accumulation of head to tail concatemers in nuclei of infected cells and their role in the generation of the four isomeric arrangements of viral DNA. J. Virol. **29**:448–457.
8. **Ladin, B. F., M. L. Blankenship, and T. Ben-Porat.** 1980. Replication of herpesvirus DNA. V. Maturation of concatemeric DNA of pseudorabies virus to genome length is related to capsid formation. J. Virol. **33**:1151–1164.
9. **Ladin, B. F., S. Ihara, H. Hampl, and T. Ben-Porat.** 1982. Pathway of assembly of herpesvirus capsids: an analysis using DNA$^+$ temperature sensitive mutants of pseudorabies virus. Virology **116**:544–561.
10. **Locker, H., and N. Frenkel.** 1979. The *Bam*I, *Kpn*I, and *Sal*I restriction enzyme maps of the DNAs of herpes simplex virus strains Justin and F: occurrence of heterogeneities in defined regions of the viral DNA. J. Virol. **32**:429–441.
11. **Locker, H., and N. Frenkel.** 1979. Structure and origin of defective genomes contained in serially passaged herpes simplex virus type 1 (Justin). J. Virol. **29**:1065–1077.
12. **Marinus, M. G.** 1973. Location of DNA methylation genes on the Escherichia coli K-12 genetic map. Mol. Gen. Genet. **127**:47–55.
13. **Mocarski, E. S., L. P. Deiss, and N. Frenkel.** 1985. The nucleotide sequence and structural features of a novel U_S-*a* junction present in a defective herpes simplex virus genome. J. Virol. **55**:140–146.
14. **Mocarski, E. S., and B. Roizman.** 1981. Site-specific inversion sequence of the herpes simplex virus genome: domain and structural features. Proc. Natl. Acad. Sci. USA **78**:7047–7051.
15. **Mocarski, E. S., and B. Roizman.** 1982. Structure and role of the herpes simplex virus DNA termini in inversion, circularization and generation of virion DNA. Cell **31**:89–97.
16. **Mocarski, E. S., and B. Roizman.** 1982. Herpesvirus-dependent amplification and inversion of cell-associated viral thymidine kinase gene flanked by viral *a* sequences and linked to an origin of viral DNA replication. Proc. Natl. Acad. Sci. USA **79**: 5626–5630.
17. **Poffenberger, K. L., and B. Roizman.** 1985. A non-inverting genome of a viable herpes simplex virus. I. Presence of head-to-tail linkages in packaged genomes and requirements for circularization after infection. J. Virol. **53**:587–595.
18. **Rao, R. N., and S. G. Rogers.** 1979. Plasmid pKC7: a vector containing ten restriction endonuclease sites suitable for cloning DNA segments. Gene **7**:79–82.
19. **Roizman, B.** 1979. The structure and isomerization of herpes simplex virus genomes. Cell **16**:481–494.
20. **Sheldrick, P., and N. Berthelot.** 1974. Inverted repetitions in the chromosome of herpes simplex virus. Cold Spring Harbor Symp. Quant. Biol. **39**:667–678.
21. **Southern, E. M.** 1975. Detection of specific sequences among DNA fragments separated by gel electrophoresis. J. Mol. Biol. **98**:503–517.
22. **Spaete, R. R., and N. Frenkel.** 1982. The herpes simplex virus amplicon: a new eucaryotic defective-virus cloning-amplifying vector. Cell **30**:295–304.
23. **Spaete, R. R., and N. Frenkel.** 1985. The herpes simplex amplicon. III. Analysis of cis replication functions. Proc. Natl. Acad. Sci. USA **82**:694–698.
24. **Stow, N. D.** 1982. Localization of an origin of DNA replication within the TR_S/IR_S repeated region of the herpes simplex virus type 1 genome. EMBO J. **1**:863–867.
25. **Stow, N. D., and E. C. McMonagle.** 1983. Characterization of the TR_S/IR_S origin of DNA replication of herpes simplex virus type 1. Virology **130**:427–438.
26. **Stow, N. D., E. C. McMonagle, and A. J. Davison.** 1983. Fragments from both termini of the herpes simplex virus type 1 genome contain signals required for the encapsulation of viral DNA. Nucleic Acid Res. **11**:8205–8220.
27. **Varmuza, S. L., and J. R. Smiley.** 1985. Signals for site-specific cleavage of herpes simplex virus DNA: maturation involves two separate cleavage events at sites distal to the recognition site. Cell **41**:793–802.
28. **Vlazny, D. A., and N. Frenkel.** 1981. Replication of herpes simplex virus DNA: localization of replication recognition signals within defective virus genomes. Proc. Natl. Acad. Sci. USA **78**:742–746.
29. **Vlazny, D. A., A. D. Kwong, and N. Frenkel.** 1982. Site specific cleavage/packaging of herpes simplex virus DNA and the selective maturation of nucleocapsids containing full length viral DNA. Proc. Natl. Acad. Sci. USA **79**:1423–1427.
30. **Wagner, M. J., and W. C. Summers.** 1978. Structure of the joint region and the termini of the DNA of herpes simplex virus type 1. J. Virol. **27**:374–387.